V.A.Romaka, *doc. techn. sciences, professor*[1]
L.P. Romaka, *cand. chem. of science*[2]
Yu.V. Stadnyk, *cand. chem. of science*[2]
V.V.Romaka, *doc. techn. sciences, cand. chem. of science, dochent* [1,3]
A.M. Horyn, *cand. chem. of science*[3],
I.M. Romaniv[2]

[1]National University "Lvivska Politechnika", 12, S. Bandera Str., Lviv, 79013, Ukraine;
e-mail: vromaka@polynet.lviv.ua
[2]Ivan Franko National University of Lviv, 6, Kyryla and Mefodiya Str., Lviv, 79005, Ukraine;
e-mail: lyubov.romaka@lnu.edu.ua,
[3]Institute for Solid State Research, IFW-Dresden, Helmholtzstr. 20, 01069 Dresden, Germany.

FEATURES OF STRUCTURAL, ENERGY, ELECTROKINETIC AND MAGNETIC CHARACTERISTICS OF $Ti_{1-x}Sc_xCoSb$ THERMOELECTRIC MATERIAL

The crystalline and electronic structures, electrokinetic, energy and magnetic characteristics of the $Ti_{1-x}Sc_xCoSb$ thermoelectric material were investigated in the ranges T=80–400 K, x=0.005–0.15. Mechanisms of simultaneous generation of structural defects of the acceptor and donor nature were established. It was shown that the structure of TiCoSb basic compound is defective, comprising defects of the donor and acceptor nature as a result of location in the tetrahedral voids of additional Co atoms and the presence of vacancies at the 4a position of Ti atoms. The introduction of impurity Sc atoms into TiCoSb compound by substitution at the 4a position of Ti atoms generates the acceptor defects, and the ratio of concentrations of available donors and generated acceptors determines the position of the Fermi level ε_F, type, and the mechanisms of conduction for $Ti_{1-x}Sc_xCoSb$. Bibl. 12, Fig. 8.*
Key words: electronic structure, electrical resistivity, Seebeck coefficient.

Introduction

Semiconductor thermoelectric materials based on the *TiCoSb* half-Heusler phase have high efficiency of thermal energy into electrical energy conversion [1–8]. In the above mentioned works, the optimization of the parameters of thermoelectric materials to obtain the maximum values of thermoelectric figure of merit [9] was performed by doping the *TiCoSb* semiconductor, owing to which the resulting materials become heavilydoped and strongly compensated semiconductors [10].

The authors of [1–8] predicted that structural defects of the donor nature will be generated in the crystals of $TiCo_{1-x}Ni_xSb$, $TiCo_{1-x}Cu_xSb$, $Ti_{1-x}V_xCoSb$ and $Ti_{1-x}Mo_xCoSb$ semiconductor solid solutions, since *Ni*($3d^8 4s^2$) and *Cu* ($3d^{10}4s^1$) atoms have more 3*d*-electrons than *Co*($3d^7 4s^2$), and *V* ($3d^3 4s^2$) and *Mo*($4d^5 5s^1$) atoms have more 3*d*-electrons than *Ti* ($3d^2 4s^2$). However, in the course of experimental studies, it was found that the results of simulating the energy and kinetic characteristics of the above materials do not agree with the (experimental) measurement results. Such a discrepancy does not allow predicting and obtaining material with pre-assigned characteristics, due to which they were excluded from the number of promising thermoelectric

materials. Inparticular, introductionof *V*, *Mo* and *Ni* atoms in to the structure of *TiCoSb* compound was accompanied by a simultaneous generation of structural defects of the acceptor and donor nature whose ratios determine the kinetic properties of thermoelectric material.

The question arises as to thenature of the acceptors in the above semiconductors.

The authors of [5] assumed that the structure of *TiCoSb* basic semiconductor is defective and comprises at the 4*a* position of *Ti* atoms the vacancies which will be further denoted by, which, in fact, generates acceptors.Moreover, it was notex cluded that impurity atoms will occupy other positions which will also generate acceptors. For instance, on introducing to the structure of *TiCoSb* compound of *V* atoms by substituting at the 4*a* position of *Ti* atoms, which generates donors, there may beal so a simultaneous partial occupation by *V* atoms of the 4*c* crystallographic position of *Co* atoms, which will result in generating structural defects of the acceptor nature (*V* atom has a smaller number of 3*d*-electrons than *Co* atom).

The importance of understanding the structural and energy features of *TiCoSb* basic semiconductor is crucial because it gives a vision of ways to optimize the characteristics of a thermoelectric material by doping with a certain type and concentration of impurities. After all, a prerequisite for achieving maximum efficiency of thermal into electrical energy conversion is doping of material with a type of impurity that coincides with the type of majority carriers of the basic semiconductor array, when the Fermi level ε_F approaches the percolation level of the continuous energy band [11].

In this context, it is interesting to investigate $Ti_{1-x}Sc_xCoSb$ thermoelectric material obtained by substituting *Ti* atoms with *Sc* atoms ($3d^14s^2$) at the 4*a* position. In this case, structural defects of the acceptor nature must be generated in the crystal, since *Sc* atom has fewer *3d*-electrons. In turn, electrokinetic studies will confirm whether a solid substitutional solution is being realized, that is, whether the conductivity type of $Ti_{1-x}Sc_xCoSb$semiconductor will change from electron to hole. The investigations pursued will give insight into the nature of defects of *TiCoSb*basic semiconductor, which will make the process of optimization of the characteristics of thermoelectric material predictable.

Investigation procedures

The object to be investigated included crystalline structure, electronic density distribution (DOS), the magnetic, thermodynamic, kinetic and energy characteristics of $Ti_{1-x}Sc_xCoSb$. The samples of $Ti_{1-x}Sc_xCoSb$ so lid solution were sun the sized by melting the chargeo finitial components in the electrical coven in the inerter go at most here with subsequent homogenizing annealing for 720 hours at a temperature of 1073 K. Diffraction data arrays were obtained with the use of Guinier-Huberpowder diffractometer (imageplatesystem, $CuK\alpha_1$ radiation). Crystallographic parameters were calculated by means of Fullprof program [12]. The chemical and phase compositions of the samples were controlled by microprobe analyzer (EPMA, energy-dispersive *X* – ray analyzer). The electronic structure of $Ti_{1-x}Sc_xCoSb$ was simulated by the Green-function method (the Korringa-Kohn-Rostoker (KKR) method) in coherent potential approximation (CPA) and local density approximation (LDA) [13]. For calculations by KKR method use was made oflicensed soft ware AkaiKK at the 4*a* position R and SPR-KKR in LDA for Moruzzi-Janak-Williams (MJW) exchange-correlation potential with parameterization [14]. The Brillouin zone was broken into 1000 *k*-points which were used for simulation of energy characteristics by calculating DOS. The width of the energy window was 22 e *V* and was chosen to capture all semi-corestates of *p*-elements. For calculations by linear muffin-tin orbital (LMTO) use was made of full potential (FP) in the representation of plane waves. The LDA approximation with MJW parameterization was also use dasex change-correlation potential. The accuracy of calculating the position of the Fermi level ε_F= ±6meV. The temperature and concentration dependences of the electrical resistivity (ρ) and the Seebeck coefficient (α) with respect to copper and magnetic susceptibility (χ) (Faraday's method) of $Ti_{1-x}Sc_xCoSb$ samples in the

ranges:
T=80–400 K, $N_A^V \approx 9.5 \cdot 10^{19}$ cm^{-3}–$1.9 \cdot 10^{21} \cdot$cm^{-3} (x=0.005–0.10).

However, at temperatures T> 400 K, the solubility of *Sc* atoms increases, and the change in the free energy values *ΔG (x)* (Helmholtz potential) at a temperature T = 800 K passes through the minimum in the concentration range x≈0.35 (Fig. 1a, curve 5). Therefore, the compositions of $Ti_{1-x}Sc_xCoSb$, x = 0–0.15 samples under study are within the solubility range, as also evidenced by the absence of extraneous phases therein.

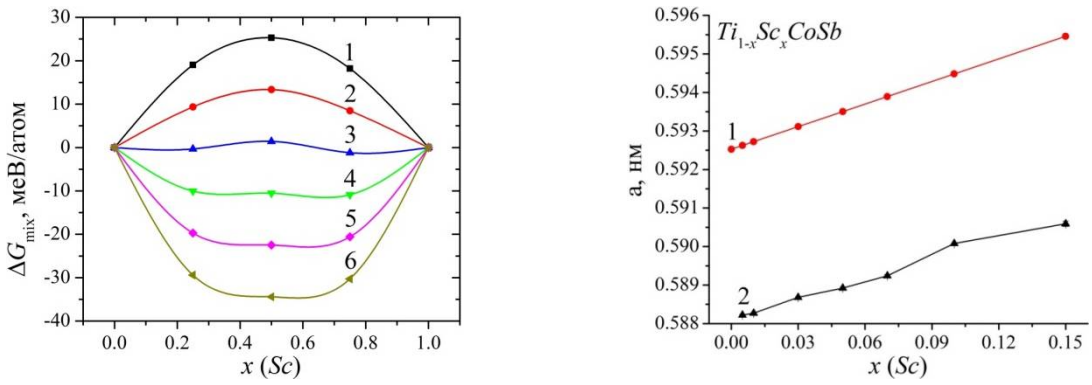

a *b*

Fig. 1. Change in the values of thermodynamic potential ΔG(x) at different temperatures (a): 1 – 0 K; 2 – 200 K; 3 – 400 K; 4 – 600 K; 5 – 800 T; 6 – 1000Kand unit cell period a(x) of $Ti_{1-x}Sc_xCoSb$: 1 – simulation, 2 – experiment(b)

Taking into account that the atomic radius of *Sc* (rSc = 0.164 nm) is larger than that of *Ti* (rTi = 0.146 nm), it is logical to increase the values of the elementary cell period *a*(x) of $Ti_{1-x}Sc_xCoSb$ (Fig. 1b). Such a behavior of the value of period *a(x)* may indicate the realization of a solid $Ti_{1-x}Sc_xCoSb$ substitutional solution and at the 4*a* position of *Ti* atoms structural defects of the acceptor nature will be generated. In so doing, in the band gap ε_g of semiconductor solid solution $Ti_{1-x}Sc_xCoSb$ the impurity acceptor zone ε_A^{Sc} will be formed.

The refinement of the crystalline structure of the $Ti_{1-x}Sc_xCoSb$ in vestigated phases allowed us to obtain the values of the Bragg discrepancy factor (R_{Br}) between the model representation of the structure and the experimental results, which showed high accuracy and quality of the simulation process, in particular: R_{Br}= 3% for x = 0.005, R_{Br} = 1.5% for x = 0.03, R_{Br} = 2.6% for x = 0.05, R_{Br} = 3.5% for x = 0.07 and R_{Br} = 3.7% for x = 0.10. With regard to the small number of impurity *Sc* atoms dissolved in the *TiCoSb* compound array, and the low accuracy of the X-ray method, we were unable to detect any other structural changes in structural studies, such as the occupation by impurity atoms of other crystallographic positions or vacancies.

We also simulated a change in the values of the unit cell period *a*(*x*) of $Ti_{1-x}Sc_xCoSb$ provided that all crystallographic positions of *TiCoSb* compound are occupied in accordance with the structural type *MgAgAs* [15], and impurity *Sc* atoms will displace *Ti* atom sat the 4*a* position. If we compare the experimentally obtained change in the values of period *a*(*x*) of $Ti_{1-x}Sc_xCoSb$(Fig. 1b, curve 2) with the course of dependence *a(x)* obtained by calculations (Fig. 1*b*, curve 1), then the curves are close to parallel.The result, at first glance, is amazing. If the course of the calculated and experimentally obtained dependences *a*(*x*) of $Ti_{1-x}Sc_xCoSb$ do not coincide, then this may indicate the inability to take into account all the features of the structure when modeling. This is normal! However, the values of the periods *a*(*x*) for

TiCoSb basic compound, to which the impurity *Sc* atoms are introduced, do not essentially coincide, forming $Ti_{1-x}Sc_xCoSb$ semiconductor solid solution.

What is the reason for this and why are the experimentally obtained $a(x)$ values of *TiCoSb* less than the calculated ones?

We believe that the difference in the values of period $a(x)$ is a manifestation of vacancies in the structure of *TiCoSb* compound, which reduces its volume and, accordingly, the value of period $a(x)$. This conclusion is consistent with that previously obtained in [5]. If we conventionally combine the values of the period $a(x)$ of *TiCoSb* compound obtained experimentally (Fig. 1b, curve 2) with the value obtained by the simulation (Fig. 1b, curve 1), then the dependences $a(x)$ of $Ti_{1-x}Sc_xCoSb$ coincide within the experiment accuracy.

Consequently, structural studies of $Ti_{1-x}Sc_xCoSb$ semiconductor solid solution suggest the ordering of its crystalline structure, and substitution at the 4*a*position of *Ti* atoms with *Sc* will generate structural defects of the acceptor nature.

Research on the electronic structure of $Ti_{1-x}Sc_xCoSb$

To predict the behavior of the Fermi level ε_F, the band gap ε_g and the kinetic characteristics of $Ti_{1-x}Sc_xCoSb$, the electron density (DOS) distribution (Fig. 2) was calculated for an ordered variant of the structure in which *Ti* atoms at the 4*a*position are substituted with *Sc*.

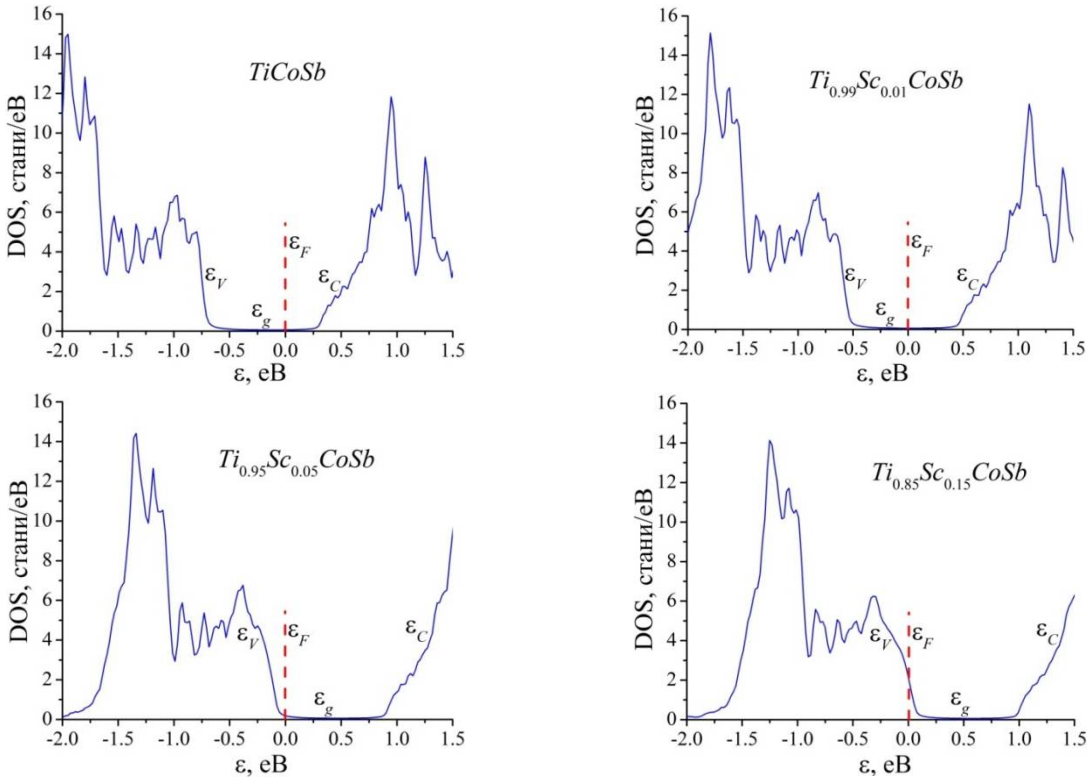

Fig. 2. Distribution of the electron density of states DOSof $Ti_{1-x}Sc_xCoSb$for the ordered structure

As can be seen from Fig. 2, in the *TiCoSb* half-Heusler phase, the Fermi level ε_F (dashed line) is located in the band gap ε_g near its middle, but closer to the percolation level of the conduction band ε_C. Since the replacement of *Ti* atoms with *Sc* generates structural defects of the acceptor nature, already at $Ti_{0.99}Sc_{0.01}CoSb$ concentration, the Fermi level ε_F will drift from the conduction band ε_C and take a position in the mid gap ε_g. At higher concentrations of the acceptor impurity, the concentration of acceptors will increase, and the Fermi level ε_F will approach and subsequently intersect the percolation level of the

valence band ε_V of $Ti_{1-x}Sc_xCoSb$: there will be a dielectric-metal conductivity transition, which is the Anderson transition [16]. Approximation of the Fermi level ε_F to the percolation level of the valence band ε_V will change the sign of the Seebeck coefficient $\alpha\ (T, x)$ from negative to positive, and the intersection by the Fermi levels ε_F of the percolation level of the valence band ε_V will change the conductivity of $Ti_{1-x}Sc_xCoSb$ semiconductor from activation to metallic [10,16]: the activation regions will disappear on the dependences ln(ρ (1 / T) and the resistance values ρ will increase with temperature. The change in the density of states at the Fermi level $g(\varepsilon_F)$ is slower.

The distribution of the electron localization function *(elf)* in $Ti_{1-x}Sc_xCoSb$ solid solution (Fig. 3) indicates that there is a strong localization in *TiCoSb* compound between *Co* and *Sb* atoms, whereas around *Ti* atoms there is a more closed spherical shell. Substitution at the 4*a*position of *Ti* atoms with *Sc* reduces the localization of the electron density around *Co* atoms in the direction of *Sc* atoms and slightly affects the electron density distribution between *Co* and *Sb* atoms.

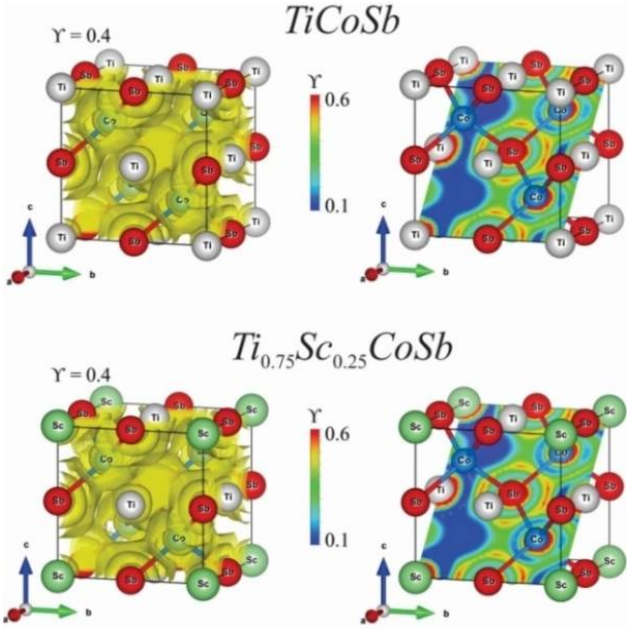

Fig. 3. Distribution of the values of electron localization function (γ=0,4) in plane [101] and electron density isosurface(0,053 e/(103 nm^3)) forTiCoSbandTi$_{0.75}$Sc$_{0.25}$C0Sb

The DOS electronic state density distribution for the ordered $Ti_{1-x}Sc_xCoSb$ structure allows simulating the behavior of the resistivity, the Seebeck coefficient α(x,T), thermoelectric power Z*, etc. (Figs. 4, 5*a*). Simulating the behavior of the Seebeck coefficient α(x,T) yields, as expected, positive values at all concentrations and temperatures, and maximum values of α(x,T) are achieved at concentration x≈0.08. In the range of concentrations of *Sc* atoms, x≈0.08–0.11, maximum values of the thermoelectric power factor Z* calc are predicted (Fig. 4b).

Fig. 5*a* shows a dependence inverse to the density of states at the Fermi level $g(\varepsilon_F)$, whose values are proportional to the electrical resistivity of the thermoelectric material $Ti_{1-x}Sc_xCoSb$. It can be seen that the dependence $1/g(\varepsilon_F)$ passes through the maximum at the concentrations of *Sc* atoms, x≈0.01, and then decreases rapidly and reaches quasi-saturation at x> 0.10.This behavior of $1/g(\varepsilon_F)$ is understandable, since the increase in the dependence on the plot x = 0–0.10 is related to the intersection by the Fermi level ε_F of the mid gap, which causes the smallest values of $g(\varepsilon_F)$ and the maximum values of the semiconductor electrical resistance. At higher concentrations of *Sc*, x > 0.01, the Fermi level ε_F will approach the

percolation level of the valence band ε_V, leading to the appearance and growth of the concentration of free holes, as well as the density of states at the Fermi level $g(\varepsilon_F)$. Experimental studies of the magnetic, kinetic, and energy characteristics of a $Ti_{1-x}Sc_xCoSb$ solid solution will show the correspondence of these calculations to the real processes in thermoelectric material.

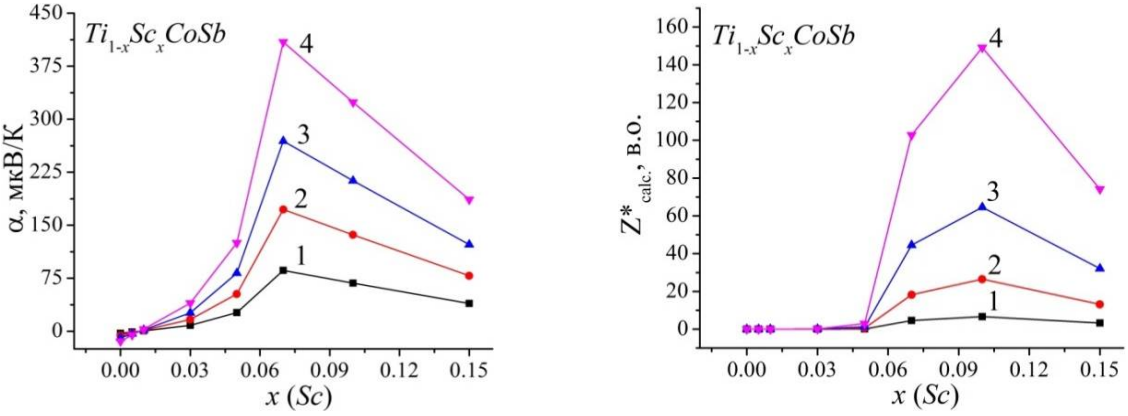

a *b*

*Fig. 4. Simulation of change in the values of the Seebeck coefficient α(x,T) at temperatures: 1 – 80 K; 2 – 160 K; 3 – 250 K; 4 – 380 K(**a**) and thermoelectric power factor $Z^*_{calc.}$(**b**) of $Ti_{1-x}Sc_xCoSb$for the ordered structure*

Research on magnetic susceptibility of $Ti_{1-x}Sc_xCoSb$

Interesting are the results of measuring magnetic susceptibility χ of thermoelectric material $Ti_{1-x}Sc_xCoSb$ (Fig. 5*b*), which are basically consistent with the results of simulating the electronic structure of a semiconductor. Studies have shown that $Ti_{1-x}Sc_xCoSb$ samples, x > 0.005, are Pauli paramagnetics in which the magnetic susceptibility χ is determined solely by electron gas and is proportional to the Fermi density of states $g(\varepsilon_F)$.

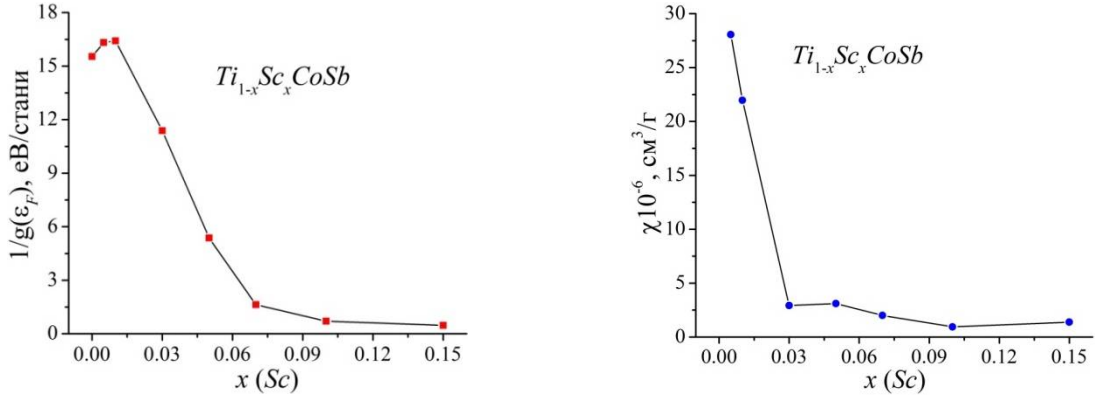

a) *b)*

Fig. 5. Simulation of change in the values $1/g(\varepsilon_F)$ (a) and experimental dependence of magnetic susceptibility χ(x) at temperature T=300 K(b) of $Ti_{1-x}Sc_xCoSb$

As can be seen from Fig. 5*b*, the dependence χ (*x*) at *x* > 0.03 rapidly changes the slope, enters the plateau and is almost unvaried up to *x* = 0.15. That is, the increase in the concentration of the acceptor impurity and the possible increase in the concentration of free holes little changes the value of the state density at the Fermi level $g(\varepsilon_F)$. Such behavior of χ (*x*) ($\chi \sim g(\varepsilon_F)$) is possible, provided that the Fermi level

ε_F intersects the percolation level of valence band ε_V $Ti_{1-x}Sc_xCoSb$ with subsequent drift over the continuous energy band, as shown by the DOS simulation results (Fig. 2).

Researchon the electrokinetic and energy characteristics of $Ti_{1-x}Sc_xCoSb$

The temperature and concentration dependences of the resistivity ρ and the Seebeck coefficient α of $Ti_{1-x}Sc_xCoSb$ are shown in Figs. 6 and 7. The dependence ln(ρ(1/*T*)) of *TiCoSb* is approximated using the well-known relation [10]:

$$\rho^{-1}(T) = \rho_1^{-1} \exp\left(-\frac{\varepsilon_1^{\rho}}{k_B T}\right) + \rho_3^{-1} \exp\left(-\frac{\varepsilon_3^{\rho}}{k_B T}\right), \quad (1)$$

where the first high-temperature term describes the activation of current carriers ε_1^{ρ}=100.6 mcV from the Fermi level ε_F to the percolation level of continuous energy bands, and the second, low-temperature term, the hopping conductivity through impurity donor states ε_3^{ρ} = 5.1 mcV. In turn, the temperature dependence of the Seebeck coefficient α(1/*T*) *TiCoSb* is approximated using the expression [16]:

$$\alpha = \frac{k_B}{e}\left(\frac{\varepsilon_i^{\alpha}}{k_B T} - \gamma + 1\right), \quad (2)$$

where γ is a parameter depending on the nature of scattering. The activation energy ε_1^{α}=214.1 mcV was calculated from the high-temperature region of the α (1/*T*) dependence, which, as shown in [17], is proportional to the amplitude of large-scale fluctuation of continuous-energy bands, and from the low-temperature region, the value of activation energy ε_3^{α}=10.2 mcV, proportional to the modulation amplitude of small-scale fluctuations of heavily doped and strongly compensated semiconductors [10,17].

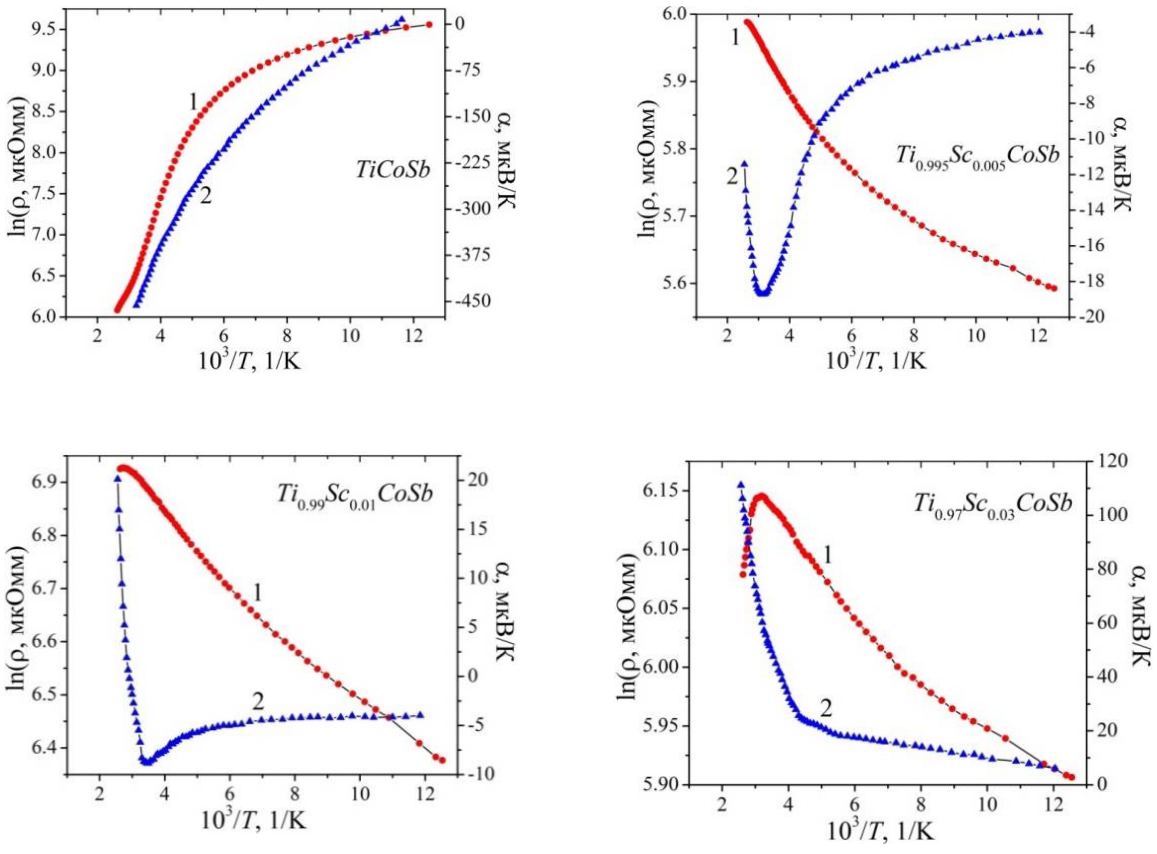

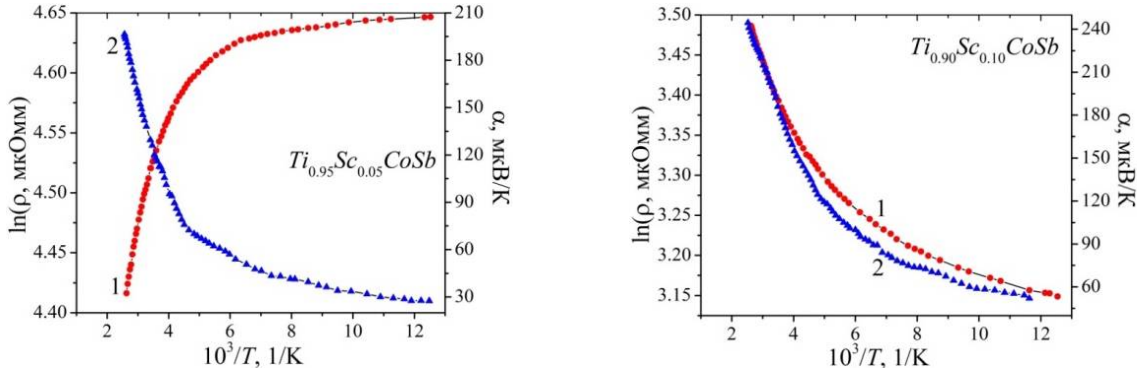

Fig. 6. Temperature dependences of electrical resistivity ln(ρ(1/T)) and the Seebeck coefficient α(1/T) of thermoelectric material$Ti_{1-x}Sc_xCoSb$.

The results obtained for *TiCoSb* coincide with those previously obtained in [1–8]. Strong compensation, i.e. close concentration of ionized acceptors and donors, is indicated by the results of studies of the Seebeck coefficient α (Fig. 6). Thus, in the temperature range *T*=80–90 K, *TiCoSb* is a hole-type semiconductor, as evidenced by the positive values of the Seebeck coefficient: $\alpha_{80\ K}$=7.75 mcV/K and $\alpha_{90\ K}$=0.71mcV/K. At higher temperatures, the sign of the Seebeck coefficient α ($\alpha_{95\ K}$ = -6.33 mcV/K) changes and electrons become the majority carriers.

Obviously, in the crystal of the *TiCoSb* compound, both donor and acceptor defects are present, generating corresponding donor and acceptor energy levels (zones) in the forbidden zone. At low temperatures, the electron energy is insufficient to flow into the conduction band ε_C (for donor ionization), and impurity acceptor states are small. A temperature of 80 K or less is sufficient for ionization of the acceptors and the holes become the majority carriers. With a rise in temperature, when donor ionization becomes possible, the concentration of electrons and their contribution to conductivity increases. Under these conditions, the Seebeck coefficient changes from positive to negative, and the Fermi level ε_F at $T_{inv.}$≈90 K crosses the mid gap ε_g.

Addition to the *TiCoSb* of the lowest concentration of *Sc* atoms in the experiment by replacing the *Ti* atoms radically changes the behavior of the resistivity *ρ* and the Seebeck coefficientα of $Ti_{0.995}Sc_{0.005}CoSb$. In the 80–350 K temperature range, the resistivity values ρ increase with a rise in temperature, and the conductivity of $Ti_{0.995}Sc_{0.005}CoSb$ is metallic. That is, the addition of the lowest concentration of *Sc* atoms in the experiment (x = 0.005) to be generated by the acceptors changed the position of the Fermi level ε_F in a way that can only cause the appearance of donors in a semiconductor. Thus, if in *TiCoSb* the Fermi level ε_F was in the band gap, then the metallization of the conductivity of $Ti_{0.995}Sc_{0.005}CoSb$ indicates that it not only approached the conduction band, but also crossed its percolation level, and electrons remain the majority carriers. This is indicated by the negative values of the Seebeck coefficient α of $Ti_{0.995}Sc_{0.005}CoSb$. This is only possible if donors of so far unknown nature are generated in a semiconductor.

The metallization of the conductivity of $Ti_{0.995}Sc_{0.005}CoSb$ does not correspond to the results of the simulation of the electronic structure. After all, it was predicted that at the smallest concentration of *Sc* acceptor impurity, the Fermi level ε_F would drift from the conduction band ε_C to the mid gap ε_g.. Therefore, in the high-temperature region of dependence ln(ρ(1/*T*)) there must be an activation region associated with the thermal throw of electrons from the Fermi level ε_F into the conduction band ε_C, and the value of the electron activation energy ε_1^{ρ} should be greater than in the case of *TiCoSb*.

The discrepancy between the simulation results and the experimental studies of the kinetic characteristics of the semiconductor at the lowest concentration of impurity *Sc*(x = 0.005) can be the result

of both the low quality of the synthesized sample and the incomplete consideration of the features of the crystalline structure of $Ti_{0.995}Sc_{0.005}CoSb$ when simulating the characteristics. However, metallographic studies of the $Ti_{1-x}Sc_xCoSb$ samples [18] established their homogeneity and correspondence between the sample composition on the surface and the charge components before synthesis.

On the other hand, the presence of extremes at the temperature of ~ 350 K on the dependences $\ln(\rho(1/T))$ and $\alpha(1/T)$ of $Ti_{0.995}Sc_{0.005}CoSb$ indicates the appearance and participation in semiconductor conduction of free holes, which caused the Fermi level ε_F to return to the band gap ε_g This result is consistent with the simulation results, which provided for the generation of acceptors in the $Ti_{1-x}Sc_xCoSb$ crystal.

At a higher acceptor concentration in the $Ti_{0.99}Sc_{0.01}CoSb$ sample, the dependence $\ln(\rho\ (1/T))$ is similar to that for the $Ti_{0.995}Sc_{0.005}CoSb$ sample, but fundamental changes occurred in the behavior of the Seebeck coefficient $\alpha(1/T)$, which reflects the dynamics of changing the ratio of electrons and holes in the conductivity of a semiconductor. Thus, in the temperature range of 80-350 K, the sign of the Seebeck coefficient is negative, and hence electrons are the majority carriers. However, as can be seen from Fig. 6, the dependence of $\alpha(1/T)$ has a minimum at a temperature of ~ 300 K, following which, with a rise in temperature, the values of the Seebeck coefficient α rapidly decrease in the absolute value and change sign at temperatures $T \geq 340$ K: holes become the majority carriers in $Ti_{0.99}Sc_{0.01}CoSb$. The positive values of the Seebeck coefficient α indicate to this.

This behavior of the Seebeck coefficient is understandable and predictable, since the substitution of *Ti* atoms by *Sc* atoms generates in the crystal structural defects of the acceptor nature. In *TiCoSb* at high temperatures, when all structural defects of both the donor and acceptor nature are ionized, the sign of the Seebeck coefficient α was negative, indicating the predominance of defects of the donor nature over the acceptor. Thus, the substitution of *Ti* atoms with *Sc* at $x = 0.005$ did not radically alter the ratio of donors and acceptors in favor of the latter. However, even at $x = 0.01$ and all higher concentrations of impurity *Sc* atoms introduced into the structure of the *TiCoSb* compound, the number of structural defects of the acceptor nature is outweighed by the number of donors, as indicated by the positive values of the Seebeck coefficient α of $Ti_{1-x}Sc_xCoSb$ at temperatures of 80–400 K. Hence, in $Ti_{0.995}Sc_{0.005}CoSb$ and $Ti_{0.99}Sc_{0.01}CoSb$ semiconductors, electrons and holes are simultaneously involved in electrical conductivity, the relationship between which (compensation ratio) varies with temperature.

The dependences $\ln(\rho\ (1/T))$ of $Ti_{1-x}Sc_xCoSb$ reflect the dynamics of changing the position of the Fermi level ε_F with respect to the continuous energy bands. Thus, in $Ti_{0.97}Sc_{0.03}CoSb$ in the temperature range T= 80–320, the Fermi level ε_F is in the valence band ε_V, as evidenced by both the positive values of the Seebeck coefficient α and the metallic type of conductivity (the resistivity values increase with a rise in temperature). The presence of an extremum on the dependence $\ln(\rho\ (1/T))$ at the temperature $T\approx320$ K and the formation of the activation region with its growth shows that the Fermi level ε_F left the valence band ε_V and settled in the band gap ε_g of the semiconductor. This may occur if the donors present in the crystal are ionized, but their concentration is insufficient to change the type of conductivity.

At even higher concentrations of *Sc*($x \geq 0.05$), the number of structural defects of the acceptor nature generated in the crystal far exceeds the number of donors, which leads to the entry of the Fermi level ε_F into the valence band ε_V. This is indicated by positive values of the Seebeck coefficient α - free holes are the majority carriers, and the conductivity is metallic in nature.

Changes in the values of the resistivity $\rho(x,T)$ and the Seebeck coefficient $\alpha(x,T)$ of the $Ti_{1-x}Sc_xCoSb$ semiconductor at different temperatures (Fig. 7) complement the considerations regarding the nature of the current carriers.

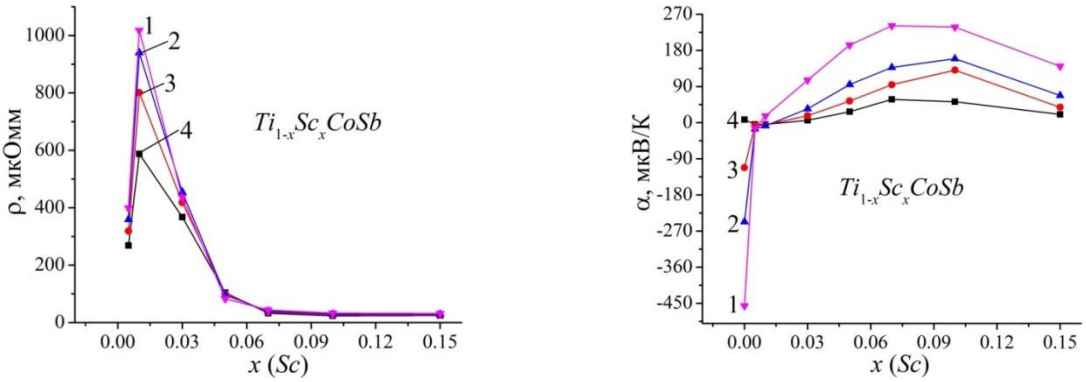

a *b*

Fig. 8. Change in the values of electrical resistivity ρ(x,T) (a) and the Seebeck coefficientα (x,T) (b) of $Ti_{1-x}Sc_xCoSb$ atdifferent temperatures: 1 – 80 K, 2 –160 K, 3 –250 K, 4 –380 K

The increase in the concentration of impurity *Sc* atoms in the structure of the *TiCoSb* compound from $x = 0.005$ to $x = 0.01$ is accompanied by an increase in the resistivity values, for example, at a temperature $T = 80$ K, from ρ ($x = 0.005$) = 268.4 mcOhm to ρ (x =0.01) = 587.8 mcOhm (which does not correspond to the data in Fig. 8a, this data seems to be for $T = 380$ K). This behavior of ρ (x,T) is caused by a decrease in the concentration of free electrons upon their "freezing" into impurity acceptor states, which would logically lead to an increase in resistance values. In so doing, the majority carriers up to temperatures $T \leq 350$ K are electrons, as indicated by the negative values of the Seebeck coefficient α(x,T).At higher temperatures, the concentration of free holes in the $Ti_{0.99}Sc_{0.01}CoSb$ sample becomes larger than of electrons, and the sign of the Seebeck coefficient α(x, T) is positive (Fig. 7). It can be stated that the $Ti_{0.99}Sc_{0.01}CoSb$ semiconductor is heavily doped and fully compensated when the concentrations of ionized donors and acceptors are close, and the Fermi level ε_F is located in the mid gap ε_g. This conclusion is in complete agreement with the results of the electronic structure calculation for the case of the $Ti_{0.99}Sc_{0.01}CoSb$ semiconductor (Fig. 2).

At higher concentrations of impurity *Sc*, the values of the resistivity *ρ(x,T) of Ti1-xScxCoSb* decrease rapidly, and at concentrations $x \geq 0.06$ this change is already insignificant. At these $Ti_{1-x}Sc_xCoSb$ concentrations, the majority carriers are free holes, as indicated by the positive values of the Seebeck coefficient α(x,T) (Fig. 7).Therefore, a sharp decrease in the values of ρ(x,T) in the concentration range $0.01 \leq x \leq 0.08$ is associated with the intersection by the Fermi level ε_F of the mid gap ε_g and the approach to the percolation level of valence band ε_V, which will be crossed at $x \approx 0.08$, causing a fast increase in the concentration of free holes as the ionization energy of acceptors decreases. The intersection by the Fermi level ε_F of the percolation level of the valence band ε_V and the motion in this zone make no significant contribution to the change in the concentration of holes, which causes quasi saturation of the dependence ρ(x,T) at concentrations $x \geq 0.08$.

Thermoelectric power factor of $Ti_{1-x}Sc_xCoSb$

We mentioned above that in thermoelectric semiconductor material a prerequisite for achieving maximum efficiency of thermal into electrical energy conversion is doping the material with a type of impurity that coincides with the type of majority carriers of the basic semiconductor array, and the Fermi level ε_F approaches the band of continuous energies. In this case, the values of electrical conductivity σ(x,T) will be already high due to the appearance of a large number of free current carriers, and the values of the Seebeck coefficient α(x,T) will be even higher.

As can be seen from Fig. 8, in the case of thermoelectric material $Ti_{1-x}Sc_xCoSb$, the above conditions are achieved at concentrations $x \approx 0.08$–0.10, and the values of thermoelectric power factor Z* are

maximum. In this context, it is appropriate to refer to the results of simulating the behavior of the thermoelectric power factor Z* calc. $Ti_{1-x}Sc_xCoSb$ (Fig. 4*b*), which almost coincide with the results of experimental measurements. The obtained result confirms the promising outlook of thermoelectric material $Ti_{1-x}Sc_xCoSb$, and further studies of thermal conductivity processes will allow establishing the conditions for obtaining the maximum efficiency of thermal into electrical energy conversion.

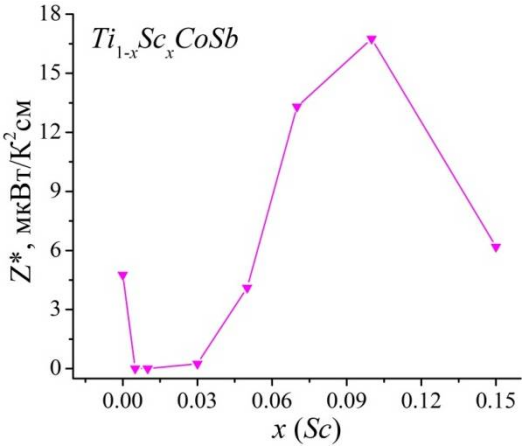

Fig. 8. Change in the values of thermoelectric power factor Z of $Ti_{1-x}Sc_xCoSb$ at T=380 K*

Therefore, kinetic studies of the $Ti_{1-x}Sc_xCoSb$ semiconductor solid solution showed that, at low concentrations of impurity *Sc* atoms, there is a discrepancy between the results of electronic structure simulation and experimental measurements. Since we optimize thermoelectric characteristics by doping the *TiCoSb* basic semiconductor, it is crucial to understand the characteristics of its crystalline and electronic structures. After all, any compound or semiconductor solid solution only then becomes a thermoelectric material when their structural, energy, kinetic, etc. the characteristics will be clear and predictable. In other words, when investigating $Ti_{1-x}Sc_xCoSb$, we are required to identify the causes that cause unpredictable behavior of the characteristics.

It can be assumed that the discrepancy in the results observed in $Ti_{1-x}Sc_xCoSb$ thermoelectric material is due to an incomplete understanding of the spatial arrangement of atoms and their impurity energy levels generated in the *TiCoSb* source compound. Below we examine this problem in more detail.

Features of the electronic and crystal in structures of *TiCoSb* compound

In order to refine the crystalline and electronic structure of *TiCoSb* compound, electron density distribution (DOS) simulations were carried out under different variants of occupying by atoms of crystallographic positions, as well as occupying by atoms of tetrahedral voids in the structure (Fig. 9), which make up ~ 24% of the unit cell volume [6,7]. After all, there is a cause-effect relationship between the crystalline and electronic structures. Thus, to calculate the energy of an electron in the first Brillou in zone, one must know the spatial location of the atoms or their absence (vacancies) at the unit cell nodes. On the other hand, the slightest structural changes affect the local symmetry and DOS values. Therefore, the adequacy of the results of simulating the electronic structure of a semiconductor and the results of experimental studies, such as kinetic and/or energy characteristics implies that the model of its structure is adequate to spatial arrangement of atoms in the crystal. That is why the results of the calculation of the electronic structure in comparison with simulation results make it possible to obtain information about the crystal structure, which is not available for x-ray methods of investigation [6].

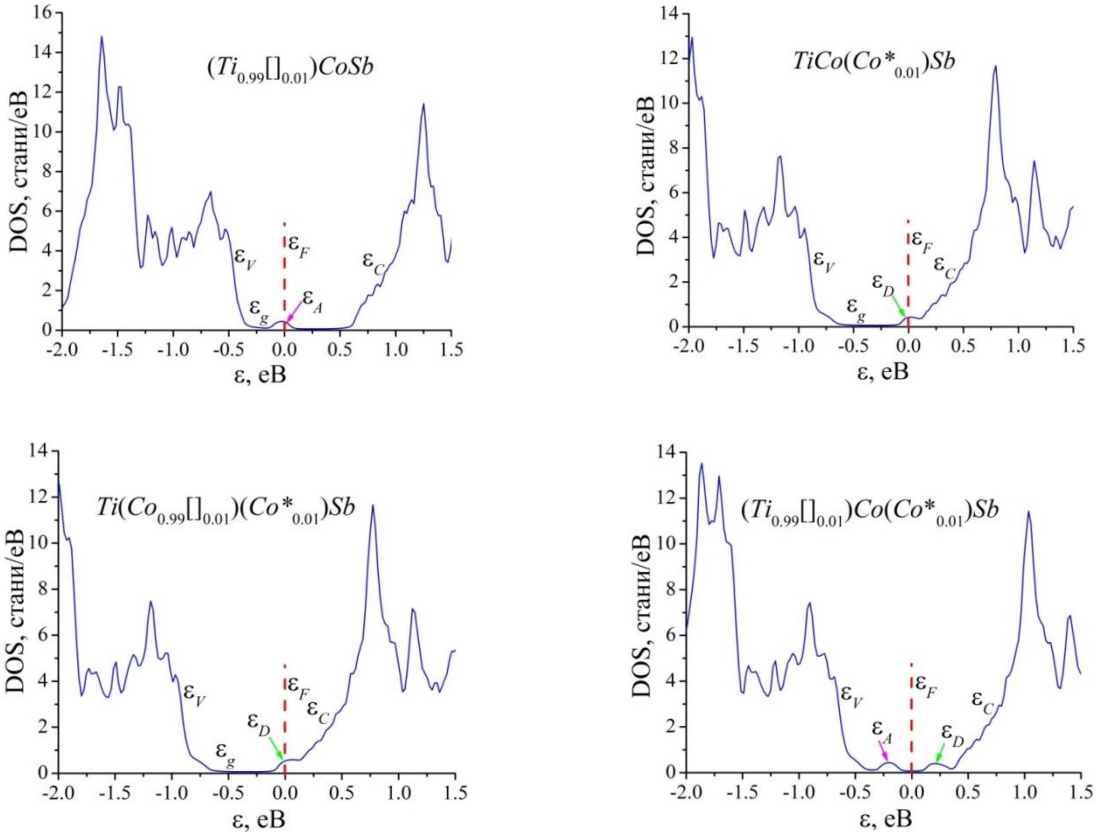

Fig. 9. Calculation of the distribution electron density of states (DOS) of TiCoSb compound for different variants of spatial arrangement of atoms.

Let us analyze the results of calculating DOS of *TiCoSb* compound for several variants (Fig. 9).

a). In the case when vacancies are present at the 4*a*crystallographic position of *Ti* atoms, which are ~ 1 at. % of all *Ti* atoms, the compound formula takes the form: $(Ti_{0.99(0.01)})CoSb$. The resulting structural defect has an acceptor nature, and an impurity acceptor level (band) ε_A, appears in the band gap ε_g of the semiconductor near the valence band ε_V, which fixes the position of the Fermi level ε_F (Fig. 9). We will obtain a model of the electronic structure of a doped hole-type semiconductor with a conductivity type. This conclusion coincides with the results of [5]. Adding *Sc* ($3d^14s^2$) impurity atoms to the structure of the semiconductor $(Ti_{0.99(0.01)})CoSb$ by occupying the 4*a* crystallographic position of *Ti*($3d^24s^2$) will have the following consequences:

- generation of structural defects of the acceptor nature as a result of substitution of *Ti* atoms, since the *Sc* atom has a smaller number of 3*d* electrons;

- a decrease in the concentration of structural defects of the acceptor nature present in the crystal upon occupation by *Sc* atoms of vacancies.

As a result, we obtain a hole-type conductivity semiconductor $Ti_{1-x}Sc_xCoSb$.This variant of the spatial arrangement of atoms does not correspond to the given experimental results.

b). If additional *Co** atoms (~ 1 at.%) occupy the tetrahedral voids of the structure (internode) of the *TiCoSb* compound, its formula will take the form $TiCo(Co^*_{0.01})Sb$. We obtain a classical doped semiconductor of electronic conductivity type, in the band gap of which an impurity donor level (band) ε_D appeared, which fixes the position of the Fermi level ε_F (Fig. 9).Now the addition of *Sc* impurity atoms to

the structure of the *TiCo (Co*$_{0.01}$) Sb* semiconductor in the manner described above will generate structural defects in the acceptor nature. As the concentration of impurity *Sc* atoms increases, the degree of compensation increases, and the Fermi level εF drifts from the conduction band ε_C through the middle of the band gap ε_g to the valence band ε_V.. This will change the conductivity type of the semiconductor from electron to hole.

This variant of the crystalline and electronic structures of the *TiCoSb* compound does not fully reflect the results of the experiment because it does not answer the question of the absence of activation sites on the dependence $\ln(\rho(1/T))$ at concentrations when the Fermi level ε_F departs from the conduction band ε_C and approaches the valence band ε_V.

c). The presence of 1% of vacancies at the *4c* position of *Co* atoms and the location of 1% additional *Co** atoms in tetrahedral voids of the structure is described by the formula $Ti(Co_{0.99(0.01)})(Co^*_{0.01})Sb$ (Fig. 9). In this case, structural defects of the donor nature are generated in the crystal due to the arrangement of *Co* atoms in the voids of the structure. Since *Co* atoms are involved in the formation of both the conduction band and the valence band of the semiconductor, in the presence of 1% of vacancies at the 4*c* position of *Co* atoms, there is a mutual compensation of the donor-acceptor energy levels, which explains their absence in the band gap ε_g.. That is why the energy scheme of such a spatial arrangement of atoms in their own crystallographic positions (or lack thereof) contains only the impurity donor level and is identical to the previous case *(b)* and the conclusions drawn.

d). The closest to the results of the experiment is a variant of the simultaneous presence of 1% of vacancies at the 4*a* position of *Ti* atoms and 1% of additional *Co** atoms in the tetrahedral voids of the structure, which can be described by the formula $(Ti_{0.99(0.01)})Co(Co^*_{0.01})Sb$ (Fig. 9). In this case, vacancies at the position of *Ti* atoms generate structural defects of the donor nature, and the corresponding acceptor level (zone) ε_A appears in the band gap ε_g. In turn, additional *Co** atoms in the voids of the structure generate a structural defect of the donor nature, and in the band gap ε_g the corresponding donor level (zone) ε_D will appear. It is quite logical to locate the Fermi level ε_F between the generated energy states of the donor and acceptor nature. The slightest changes in the ratio between defects in the acceptor and donor nature of the semiconductor, generated, for example, by different modes of thermal annealing of the samples and their cooling, the purity of the initial components during synthesis, etc., will cause a change in the position of the Fermi level ε_F relative to energy levels inε_g. For this reason, in the temperature range $T = 80$–90 K *TiCoSb* is a semiconductor of the hole type of conductivity, as evidenced by the positive values of the Seebeck coefficient α, and at higher temperatures its sign changes and electrons are now the majority carriers (Fig. 6,7*b*).

The addition of impurity *Sc* atoms to such a semiconductor by substitution at the 4*a* position of the *Ti* atoms generates structural defects of the acceptor nature, which initially will increase the degree of compensation and, as a consequence, lead to an increase in the resistivity ρ (x, T) (Fig. 7a). And only at concentrations of impurities *Sc*, $x \geq 0.03$, the Fermi level ε_F is located in the impurity acceptor zone ε_A^{Sc}, as indicated by the positive values of the Seebeck coefficient$\alpha(x,T)$ (Fig. 7*b*) at all temperatures and the presence of high-temperature of the activation region on the dependence of $\ln(\rho\ (1\ /\ T))$ (Fig. 6).

Therefore, doping the *TiCoSb* semiconductor with *Sc* acceptor impurities introduced into the structure by substitution at the 4*a* position of the *Ti* atoms made it possible to detect defects of the donor nature in the structure of the *TiCoSb* base compound as a result of the occupation by *Co** atoms of tetrahedral voids in the structure, which gave rise to a corresponding donor level (zone) ε_D in the band gap ε_g. The ratio of concentrations of the donor and acceptor levels present in the *TiCoSb* compound structure determines the location of the Fermi ε_F level in the semiconductor, and doping with its acceptor impurities will change the mechanisms and type of conductivity of $Ti_{1-x}Sc_xCoSb$.

Conclusions

1. The result of a comprehensive study of crystalline and electronic structures, kinetic, energy, and magnetic characteristics of the *Ti1-xScxCoSb* thermoelectric material is establishment of the nature of structural defects of the donor and acceptor nature. It is shown that structural defects of the donor and acceptor nature are present in the *TiCoSb* base compound as a result of the location in the tetrahedral voids of the structure of additional *Co** atoms and the presence of vacancies at the 4*a*crystallographic position of *Ti* atoms. Introduction to *TiCoSb* compound of impurity *Sc* atoms by substitution at the 4*a* position of *Ti* atoms generates structural defects of the acceptor nature, and the ratio in $Ti_{1-x}Sc_xCoSb$ of concentrations of available defects of the donor and acceptor nature determines the location of the Fermi level ε_F and the mechanisms of conductivity.
2. The work was performed in the frame work of grant of the Ministry of Education and Science of Ukraine № 0118U003609.

References

1. Romaka L. P., Shelyapina M. G., Stadnyk Yu. V., Fruchart D.,Hlil E. K., Romaka V. A. (2006). Peculiarity of metal – insulator transition due to composition change in semiconducting $TiCo_{1-x}Ni_xSb$ solid solution. I. Electronic structure calculations.*J. Alloys Compd.*, 414, 46–50.
2. Stadnyk Yu. V., Romaka V. A., Shelyapina M. G., Gorelenko Yu. K., Romaka L. P., Fruchart D., Tkachuk A. V., Chekurin V. F. (2006). Impurity band effecton $TiCo_{1-x}Ni_xSb$ conduction. Donorimpurities. *J. Alloys Compd.*, 421, 19–23.
3. Romaka V. A., Stadnyk Yu. V., Frushart D., Tobola J., Gorelenko Yu. K., Romaka L. P., Chekurin V. F., Horyn A. M. (2007). Features of doping the *p-TiCoSb* in termetallic semiconductor with a *Cu* donorimpurity. 1. Calculation of electron structure. *Ukr. J. Phys*., 52(№5), 453–457.
4. Romaka V. A., Stadnyk Yu. V., Frushart D., Tobola J., Gorelenko Yu. K., Romaka L. P., Chekurin V. F., Horyn A. M. (2007). Specific features of doping the *p-TiCoSb* in termetallic semiconductor with a *Cu* donorimpurity. 2. Experimental studies. *Ukr. J. Phys*., 52 (№7), 650–656.
5. Romaka V. A., Stadnyk Yu. V., Akselrud L. G., Romaka V. V., Frushart D., Rogl P., Davydov V. N., Gorelenko Yu. K. (2008). Mechanism of local am or phization of a heavily doped $Ti_{1-x}V_xCoSb$ in termetallic semiconductor. *Semiconductors*, 42(№7), 753–760.
6. Romaka V. A., Romaka V. V., Stadnyk Yu. V. (2011). *Intermetalichni napivprovidnyky: vlastyvosti ta zastosuvannia [Intermetallic semiconductors]*.Lviv: LvivskaPolitechnica [in Ukrainian].
7. Romaka V. V., Rogl P.F., Carlini R. and Fanciulli C. (2017).Prediction of the thermoelectric properties of half-Heuslerphases from the density functional theory. In *Alloys and Intermetallic Compounds*, Artini C. (Ed.). London–NY: Taylor & Francis Group.
8. Horyn A., Romaka V.A., Stadnyk Yu., Romaka L., RokomanukM., Krayovskyy V. (2019). *Features of Electrical Conductivity Mechanisms of the $Ti_{1-x}Mo_xCoSb$ Solid Solution*. XIV International Conference on Crystal Chemistry of Intermetallic Compounds, Collected Abstracts (Lviv, Ukraine, September 22–26, 2019).
9. Anatychuk L. I. (1979). *Termoelementy i termoelektricheskiie ustroistva. Spravochnik [Thermoelements and thermoelectric devices. Handbook]*.Kyiv: Naukovadumka [in Russian].
10. Shklovskii B.I. and Efros A.L. (1979).*Electronic properties ofdoped semiconductors.*NY: Springer, 1984; Moscow:Nauka1979 [in Russian].
11. RomakaV.A., FrushartD., StadnykYu.V., Tobola J., GorelenkoYu.K.,ShelyapinaM.G., RomakaL.P., ChekurinV.F. (2006). A condition of maximum power characteristic to intermetallic semiconductors of the *MgAgAs* structure tupe. *Semiconductors*, 40(№ 11), 1289–1395.

12. Roisnel T., Rodriguez-Carvajal J. (2001). WinPLOTR: a Windows Tool for Powder Diffraction Patterns analysis, Mater. Sci. Forum, Proc. EPDIC7 378–381, 118–123.
13. Schruter M., Ebert H., Akai H., Entel P., Hoffmann E., Reddy G.G. (1995). First-principles investigations of atomic disorder effects on magnetic and structural instabilities in transition-metal alloys.*Phys. Rev*. B 52, 188–209.
14. Moruzzi V.L., Janak J.F., Williams A.R. (1978). *Calculated electronic properties of metals (1978).* NY:PergamonPress.
15. Romaka V.V., Romaka L.P., KrayovskyyV.Ya., StadnykYu.V. (2015). *Stannides of rare earth and transition metals.*Lviv: LvivskaPolytechnika [in Ukrainian].
16. Mott N.F., Davis E.A. (1979). *Electron processes in non-crystalline materials.*Oxford: Clarendon Press.
17. RomakaV.A.,FruchartD., HlilE.K., GladyshevskiiR.E., GignouxD., RomakaV.V., KuzhelB.S. andKrayovskiiR.V. (2010). Feature so fan in termetallic *n-ZrNiSn* semiconductor heavily doped with atoms of rare-earth metals. *Semiconductors*, 44(№ 3), 293–302.
18. Stadnyk Yu., Romaka V. V.,Romaka L., Orovchik L., Horyn A. (2019). Synthesis, electrical transport, magnetic properties and electronic structure of $Ti_{1-x}Sc_xCoSb$ semiconducting solid solution. *J. Alloys Compd.*, 805, 840–846.

Submitted 18.03.2019

Ромака В.А.[1], *док. тех. наук*, *професcор*
Ромака Л.П.[2], *канд. хім. наук*
Стадник Ю.В[2], *канд. хім. наук*
Ромака В.В.[1,3], *док. тех. наук, канд. хім. наук, доц.*
Горинь А.М.[2], *канд. хім. наук*
Романів І.М.

[1]Національний університет "Львівська політехніка", вул. С. Бандери, 12, Львів, 79013, Україна; *e-mail: vromaka@polynet.lviv.ua*
[2]Львівський національний університет ім. І. Франка, вул. Кирила і Мефодія, 6, Львів, 79005, Україна; *e-mail: lyubov.romaka@lnu.edu.ua*,
[3]Інститут досліджень твердого тіла, IFW-Drezden, Гельмгольц штрасе, 20, 01069 Дрезден, Німеччина

ДОСЛІДЖЕННЯ ТЕРМОЕЛЕКТРИЧНОГО МАТЕРІАЛУ $Zr_{1-x}V_xNiSn$

Досліджено кристалічну та електронну структури, кінетичні та енергетичні характеристики термоелектричного матеріалу $Zr_{1-x}V_xNiSn$ у діапазонах: T=80–400 K, x=0.01–0.10. Встановлено механізми одночасного генерування структурних дефектів акцепторної та донорної природи, які визначають електропровідність матеріалу. Показано, що енергетично доцільним є одночасне часткове зайняття атомами V ($3d^34s^2$) позиції 4c атомів Ni ($3d^84s^2$), що генерує

структурні дефекти акцепторної природи та домішкову акцепторну зону ε^1_A, а також позиції 4а атомів Zr ($4d^25s^2$), генеруючи структурні дефекти донорної природи та домішкову донорну зону ε^2_D. Бібл. 12, Рис.8.
Ключові слова: електронна структура, електроопір, коефіцієнт термоЕРС.

Ромака В.А.[1], *док. тех. наук,* ***професcор***
Ромака Л.П.[2], *канд. хим. наук*
Стадник Ю.В[2], *канд. хим. наук*
Ромака В.В.[1,3], *док. тех. наук, канд. хим. наук, доц.*
Горынь А.М.[2], *канд. хим. наук*
Романов И.М.

[1]Национальный университет "Львовская политехника", ул. С. Бандеры, 12,
Львов, 79013, Украина, *e-mail: vromaka@polynet.lviv.ua*,
[2]Львовский национальный университет им. И. Франко,
ул. Кирилла и Мефодия, 6, Львов, 79005, Украина,
e-mail: lyubov.romaka@lnu.edu.ua,
[3]Институт исследований твердого тела, IFW-Drezden,
Гельмгольц штрассе, 2001069 Дрезден, Германия

ИССЛЕДОВАНИЕ ТЕРМОЭЛЕКТРИЧЕСКИХ МАТЕРИАЛОВ $Zr_{1-x}V_xNiSn$

Исследованы кристаллическая и электронная структуры, кинетические и энергетические характеристики термоэлектрического материала $Zr_{1-x}V_xNiSn$ в диапазонах: T = 80-400 K, x = 0.01-0.10. Установлены механизмы одновременного генерирования структурных дефектов акцепторной и донорной природы, которые определяют электропроводность материала. Показано, что энергетически целесообразно одновременное частичное занятие атомами V ($3d^34s^2$) позиции 4c атомов Ni ($3d8^4s^2$), генерирующий структурные дефекты акцепторной природы и примесную акцепторную зону, ε^1_A а также позиции 4a атомов Zr ($4d^25s^2$), генерируя структурные дефекты донорной природы и примесную донорных зону ε^2_D. Библ. 12, Рис.8.
Ключевые слова: электронная структура, электросопротивление, коэффициент термоЭДС.

References

1. Romaka L. P., Shelyapina M. G., Stadnyk Yu. V., Fruchart D.,Hlil E. K., Romaka V. A. (2006). Peculiarity of metal – insulator transition due to composition change in semiconducting $TiCo_{1-x}Ni_xSb$ solid solution. I. Electronic structure calculations.*J. Alloys Compd.*, 414, 46–50.
2. Stadnyk Yu. V., Romaka V. A., Shelyapina M. G., Gorelenko Yu. K., Romaka L. P., Fruchart D., Tkachuk A. V., Chekurin V. F. (2006). Impurity band effecton $TiCo_{1-x}Ni_xSb$ conduction. Donorimpurities. *J. Alloys Compd.*, 421, 19–23.
3. Romaka V. A., Stadnyk Yu. V., Frushart D., Tobola J., Gorelenko Yu. K., Romaka L. P., Chekurin V. F., Horyn A. M. (2007). Features of doping the *p-TiCoSb* in termetallic semiconductor with a *Cu* donorimpurity. 1. Calculation of electron structure. *Ukr. J. Phys*., 52(№5), 453–457.

4. Romaka V. A., Stadnyk Yu. V., Frushart D., Tobola J., Gorelenko Yu. K., Romaka L. P., Chekurin V. F., Horyn A. M. (2007). Specific features of doping the *p-TiCoSb* in termetallic semiconductor with a *Cu* donorimpurity. 2. Experimental studies. *Ukr. J. Phys*., 52 (№7), 650–656.
5. Romaka V. A., Stadnyk Yu. V., Akselrud L. G., Romaka V. V., Frushart D., Rogl P., Davydov V. N., Gorelenko Yu. K. (2008). Mechanism of local am or phization of a heavily doped $Ti_{1-x}V_xCoSb$ in termetallic semiconductor. *Semiconductors*, 42(№7), 753–760.
6. Romaka V. A., Romaka V. V., Stadnyk Yu. V. (2011). *Intermetalichni napivprovidnyky: vlastyvosti ta zastosuvannia [Intermetallic semiconductors]*.Lviv: LvivskaPolitechnica [in Ukrainian].
7. Romaka V. V., Rogl P.F., Carlini R. and Fanciulli C. (2017).Prediction of the thermoelectric properties of half-Heuslerphases from the density functional theory. In *Alloys and Intermetallic Compounds*, Artini C. (Ed.). London–NY: Taylor & Francis Group.
8. Horyn A., Romaka V.A., Stadnyk Yu., Romaka L., RokomanukM., Krayovskyy V. (2019). *Features of Electrical Conductivity Mechanisms of the $Ti_{1-x}Mo_xCoSb$ Solid Solution*. XIV International Conference on Crystal Chemistry of Intermetallic Compounds, Collected Abstracts (Lviv, Ukraine, September 22–26, 2019).
9. Anatychuk L. I. (1979). *Termoelementy i termoelektricheskiie ustroistva. Spravochnik [Thermoelements and thermoelectric devices. Handbook]*.Kyiv: Naukovadumka [in Russian].
10. Shklovskii B.I. and Efros A.L. (1979).*Electronic properties ofdoped semiconductors.*NY: Springer, 1984; Moscow:Nauka1979 [in Russian].
11. RomakaV.A., FrushartD., StadnykYu.V., Tobola J., GorelenkoYu.K.,ShelyapinaM.G., RomakaL.P., ChekurinV.F. (2006). A condition of maximum power characteristic to intermetallic semiconductors of the *MgAgAs* structure tupe. *Semiconductors*, 40(№ 11), 1289–1395.
12. Roisnel T., Rodriguez-Carvajal J. (2001). WinPLOTR: a Windows Tool for Powder Diffraction Patterns analysis, Mater. Sci. Forum, Proc. EPDIC7 378–381, 118–123.
13. Schruter M., Ebert H., Akai H., Entel P., Hoffmann E., Reddy G.G. (1995). First-principles investigations of atomic disorder effects on magnetic and structural instabilities in transition-metal alloys.*Phys. Rev*. B 52, 188–209.
14. Moruzzi V.L., Janak J.F., Williams A.R. (1978). *Calculated electronic properties of metals (1978).* NY:PergamonPress.
15. Romaka V.V., Romaka L.P., KrayovskyyV.Ya., StadnykYu.V. (2015). *Stannides of rare earth and transition metals.*Lviv: LvivskaPolytechnika [in Ukrainian].
16. Mott N.F., Davis E.A. (1979). *Electron processes in non-crystalline materials.*Oxford: Clarendon Press.
17. RomakaV.A.,FruchartD., HlilE.K., GladyshevskiiR.E., GignouxD., RomakaV.V., KuzhelB.S. andKrayovskiiR.V. (2010). Feature so fan in termetallic *n-ZrNiSn* semiconductor heavily doped with atoms of rare-earth metals. *Semiconductors*, 44(№ 3), 293–302.
18. Stadnyk Yu., Romaka V. V.,Romaka L., Orovchik L., Horyn A. (2019). Synthesis, electrical transport, magnetic properties and electronic structure of $Ti_{1-x}Sc_xCoSb$ semiconducting solid solution. *J. Alloys Compd.*, 805, 840–846.

Submitted 18.03.2019